Coupled Systems Mechanics, *Vol. 9, No. 3 (2020) 201-217*
DOI: https://doi.org/10.12989/csm.2020.9.3.201

Vibration analysis of nonlocal strain gradient porous FG composite plates coupled by visco-elastic foundation based on DQM

Mohammed Abdulraoof Abdulrazzaq, Ahmed K. Muhammad, Zeyad D. Kadhim and Nadhim M. Faleh*

Engineering Collage, Al-Mustansiriah University, P.O. Box 46049, Bab-Muadum, Baghdad 10001, Iraq

(Received July 29, 2019, Revised November 3, 2019, Accepted December 14, 2019)

Abstract. This paper employs differential quadrature method (DQM) and nonlocal strain gradient theory (NSGT) for studying free vibrational characteristics of porous functionally graded (FG) nanoplates coupled by visco-elastic foundation. A secant function based refined plate theory is used for mathematical modeling of the nano-size plate. Two scale factors are included in the formulation for describing size influences based on NSGT. The material properties for FG plate are porosity-dependent and defined employing a modified power-law form. Visco-elastic foundation is presented based on three factors including a viscous layer and two elastic layers. The governing equations achieved by Hamilton's principle are solved implementing DQM. The nanoplate vibration is shown to be affected by porosity, temperature rise, scale factors and viscous damping.

Keywords: composite plate; FG material; nonlocal strain gradient theory; visco-elastic foundation; DQM

1. Introduction

When the pore distribution inside the material is selected to be non-uniform, it might be defined as a functionally graded material since its properties obey some specified functions. However, the term functionally graded is not used only for non-uniform porous foams only. This term is a general term for a variety of materials in which the properties are graded and are not uniform. One example is a functionally graded (FG) material based on two components which are ceramic and metal. In fact, the properties are graded from ceramic to metal. In such gradation of material properties, porosities could be inevitable. Due to contribution of two materials in this FG material, porosities occur as a sequence of material combination defect. Many researches have been focused on such FG material based structures with the consideration of pore effect (Jabari *et al*. 2008, Chikh *et al*. 2016, Sobhy 2016, Lal *et al*. 2017, Bouderba *et al*. 2016, El-Hassar *et al*. 2016, Atmane *et al*. 2017, Alasadi *et al*. 2019, Medani *et al*. 2019, Berghouti *et al*. 2019).

A structure at nano scale could not be modeled based on well-known elasticity theory which is used for macro size structures. This shortcoming comes from the inexistence of a scale parameter in classical elasticity. Thus, non-classical or higher order elasticity theories will be utilized in order to

*Corresponding author, Ph.D., E-mail: dr.nadhim@uomustansiriyah.edu.iq

http://www.techno-press.org/?journal=csm&subpage=8 ISSN: 2234-2184 (Print), 2234-2192 (Online)

mathematically model a structure a nano scale. Such mathematical modeling is of great importance since experiments are at nano level are still difficult. As a consequence, the well-known non-local elasticity (Eringen 1983) is notably used in such mathematical modeling for structures at nano level. After this mathematical modeling, it is possible to analyze structural behaviors of beams, plates and shell having nano-dimension. Some examples are the works done by Berrabah *et al*. (2013), Zenkour and Abouelregal (2014), Aissani *et al*. (2015), Besseghier *et al*. (2015), (2017), Elmerabet *et al*. (2017), Bouadi *et al*. (2018), Yazid *et al*. (2018), Natarajan *et al*. (2012), Karami *et al*. (2018), (2019a-d), Daneshmehr and Rajabpoor (2014), Belkorissat *et al*. (2015), Semmah *et al*. (2019), Larbi Chaht *et al*. (2015). Due to the ignorance of strain gradient effect in nonlocal elasticity theory, a more general theory will be required. Strain gradients at nano-scale are observed by many researchers (Lam *et al*. 2003, Lim *et al*. 2015, Mirsalehi *et al*. 2017). Thus, nonlocal-strain gradient theory was introduced as a general theory which contains an additional strain gradient parameter together with nonlocal parameter (Fenjan *et al*. 2019, Barati and Zenkour 2017).

In this research, a thick plate model is studied based on 4 field variables (Mahi *et al*. 2015, Houari *et al*. 2016, Merazi *et al*. 2015, Younsi *et al*. 2018, Issad *et al*. 2018, Sadoun *et al*. 2018, Bouafia *et al*. 2017, Sayyad and Ghugal 2018, Daouadji *et al*. 2018). Note that classical plate model doesn't consider shear deformations for thick plates (Bourada *et al*. 2015, Draiche *et al*. 2016, Boulefrakh *et al*. 2019, Chaabane *et al*. 2019, Mahmoudi *et al*. 2019, Attia *et al*. 2018, Zarga *et al*. 2019, Meksi *et al*. 2019, Khiloun *et al*. 2019). Based on introduced plate theory, dynamic characteristics of nano-scale plates made of porous FG material exposed to thermal-hygral loads will be studied. The material is ceramic-metal with different pore distributions inside it. Nonlocal and strain gradient effects due to nano-dimension of the plate have been considered. The governing equations of the nano-dimension plate will be solved with the help of DQ approach. The obtained results will be verified with a previously published article. The dynamic characteristics of porous FG nano-size plate is shown to be dependent on applied loading, pore distribution, non-local impacts, and some other parameters.

2. Nanoplate modeling based on NSGT

In the well-known nonlocal strain gradient theory (Lim *et al*. 2015), strain gradient impacts are taken into accounting together with nonlocal stress influences defined in below relation

$$\sigma_{ij} = \sigma_{ij}^{(0)} - \nabla \sigma_{ij}^{(1)} \tag{1}$$

in such a way that stress $\sigma_{ij}^{(0)}$ is corresponding to strain components ε_{kl} and a higher order stress is related to strain gradient components $\nabla\varepsilon_{kl}$ which are (Lim *et al*. 2015):

$$\sigma_{ij}^{(0)} = \int_V C_{ijkl}\alpha_0(x,x',e_0a)\varepsilon'_{kl}(x')dx' \tag{2a}$$

$$\sigma_{ij}^{(1)} = l^2\int_V C_{ijkl}\alpha_1(x,x',e_1a)\nabla\varepsilon'_{kl}(x')dx' \tag{2b}$$

in which C_{ijkl} express the elastic properties; Also, e_0a and e_1a are corresponding to nonlocality

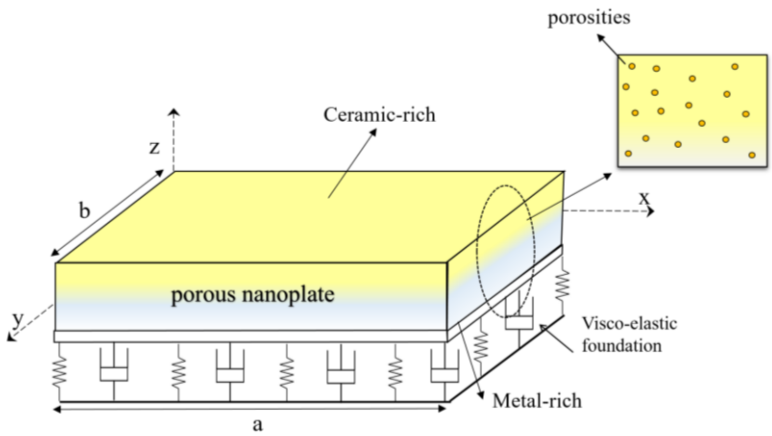

Fig. 1 Geometry of porous FG composite nanoplate coupled by visco-elastic medium

impacts and l is related to strains gradients. Whenever two nonlocality functions $\alpha_0(x,x',e_0a)$ and $\alpha_1(x,x',e_1a)$ verify Eringen's announced conditions, NSGT constitutive relation may be written as follows

$$[1-(e_1a)^2\nabla^2][1-(e_0a)^2\nabla^2]\sigma_{ij}=C_{ijkl}[1-(e_1a)^2\nabla^2]\varepsilon_{kl}-C_{ijkl}\,l^2[1-(e_0a)^2\nabla^2]\nabla^2\varepsilon_{kl} \tag{3}$$

so that ∇^2 defines the operator for Laplacian; by selecting e_1=e_0=e, above relationship decreases to

$$[1-(ea)^2\nabla^2]\sigma_{ij}=C_{ijkl}[1-l^2\nabla^2]\varepsilon_{kl} \tag{4}$$

Taking into account the temperature/humidity impact Eq. (4) might be rewritten as

$$[1-(ea)^2\nabla^2]\sigma_{ij}=C_{ijkl}[1-l^2\nabla^2](\varepsilon_{kl}-\gamma_{ij}T-\beta_{ij}C) \tag{5}$$

so that γ_{ij} and β_{ij} respectively define the temperature and humidity expansion properties.

3. Modeling FG plates having porosity

For the nanoplate shown in Fig. 1, the material distribution in FG materials may be characterized via a power-law function. FG materials are not always perfect because of porosity production in them. Existence of porosities in the FG materials may significantly change their mechanical characteristics. Depending on the type of porosity distribution, the elastic moduli E, density ρ, temperature expansion property γ and humidity expansion property β for porous FG material can be expressed in the following power-law form having material gradient index p as

$$E(z)=(E_c-E_m)\left(\frac{z}{h}+\frac{1}{2}\right)^p+E_m-\frac{\alpha}{2}(E_c+E_m) \tag{6a}$$

$$\rho(z)=(\rho_c-\rho_m)\left(\frac{z}{h}+\frac{1}{2}\right)^p+\rho_m-\frac{\alpha}{2}(\rho_c+\rho_m) \tag{6b}$$

$$\gamma(z)=(\gamma_c-\gamma_m)\left(\frac{z}{h}+\frac{1}{2}\right)^p+\gamma_m-\frac{\alpha}{2}(\gamma_c+\gamma_m) \tag{6c}$$

$$\beta(z)=(\beta_c-\beta_m)\left(\frac{z}{h}+\frac{1}{2}\right)^p+\beta_m-\frac{\alpha}{2}(\beta_c+\beta_m) \tag{6d}$$

where m and c corresponds to the metallic and ceramic sides, respectively; α defines the porosity volume fraction.

By defining exact location of neutral surface, the displacement components based on axial u, lateral v, bending w_b and shear w_s displacements may be introduced as (Fenjan *et al*. 2019)

$$u_x\left(x,y,z,t\right)=u\left(x,y,t\right)-(z-r^*)\frac{\partial w_b}{\partial x}-[\Upsilon(z)-r^{**}]\frac{\partial w_s}{\partial x} \tag{7a}$$

$$u_y\left(x,y,z,t\right)=v\left(x,y,t\right)-(z-r^*)\frac{\partial w_b}{\partial y}-[\Upsilon(z)-r^{**}]\frac{\partial w_s}{\partial y} \tag{7b}$$

$$u_z(x,y,z,t)=w(x,y,t)=w_b+w_s \tag{7c}$$

so that

$$r^*=\int_{-h/2}^{h/2}E(z)\,zdz\Big/\int_{-h/2}^{h/2}E(z)\,dz,\ r^{**}=\int_{-h/2}^{h/2}E(z)\,\Upsilon(z)dz\Big/\int_{-h/2}^{h/2}E(z)\,dz \tag{8}$$

Here, secant type shear function is employed as

$$\Upsilon(z)=z-z\sec(\frac{rz}{h})+z\sec(0.5r)[1+0.5r\tan(0.5r)],r=0.1 \tag{9}$$

Finally, the strains based on the four-unknown plate model have been obtained as

$$\begin{aligned}
\varepsilon_x&=\frac{\partial u}{\partial x}-(z-r^*)\frac{\partial^2 w_b}{\partial x^2}-[\Upsilon(z)-r^{**}]\frac{\partial^2 w_s}{\partial x^2}\\
\varepsilon_y&=\frac{\partial v}{\partial y}-(z-r^*)\frac{\partial^2 w_b}{\partial y^2}-[\Upsilon(z)-r^{**}]\frac{\partial^2 w_s}{\partial y^2}\\
\gamma_{xy}&=\frac{\partial u}{\partial y}+\frac{\partial v}{\partial x}-2(z-r^*)\frac{\partial^2 w_b}{\partial x\partial y}-2[\Upsilon(z)-r^{**}]\frac{\partial^2 w_s}{\partial x\partial y}\\
\gamma_{yz}&=g(z)\frac{\partial w_s}{\partial y},\quad \gamma_{xz}=g(z)\frac{\partial w_s}{\partial x}
\end{aligned} \tag{10}$$

Next, one might express the Hamilton's rule as follows based on strain energy (U) and kinetic energy (T)

$$\int_0^t\delta(U-T+V)dt=0 \tag{11}$$

and V is the work of non-conservative loads. Based on above relation we have

$$\begin{aligned}
\delta U=\int_V(&\sigma_{xx}\delta\varepsilon_{xx}+\sigma_{xx}^{(1)}\delta\nabla\varepsilon_{xx}+\sigma_{yy}\delta\varepsilon_{yy}+\sigma_{yy}^{(1)}\delta\nabla\varepsilon_{yy}+\sigma_{xy}\delta\gamma_{xy}+\sigma_{xy}^{(1)}\delta\nabla\gamma_{xy}\\
&+\sigma_{yz}\delta\gamma_{yz}+\sigma_{yz}^{(1)}\delta\nabla\gamma_{yz}+\sigma_{xz}\delta\gamma_{xz}+\sigma_{xz}^{(1)}\delta\nabla\gamma_{xz})dV
\end{aligned} \tag{12}$$

Note that for obtaining Eq. (12), the thickness effects have been neglected by the authors. Placing Eqs. (8) and (10) in Eq. (12) leads to

$$\delta U=\int_0^a\int_0^b[N_{xx}[\frac{\partial\delta u}{\partial x}+\frac{\partial w}{\partial x}\frac{\partial\delta w}{\partial x}]-M^b_{xx}\frac{\partial^2\delta w_b}{\partial x^2}-M^s_{xx}\frac{\partial^2\delta w_s}{\partial x^2}+N_{yy}[\frac{\partial\delta v}{\partial y}+\frac{\partial w}{\partial y}\frac{\partial\delta w}{\partial y}]$$
$$-M^b_{yy}\frac{\partial^2\delta w_b}{\partial y^2}-M^s_{yy}\frac{\partial^2\delta w_s}{\partial y^2}+N_{xy}(\frac{\partial\delta u}{\partial y}+\frac{\partial\delta v}{\partial x}+\frac{\partial w}{\partial x}\frac{\partial\delta w}{\partial y}+\frac{\partial w}{\partial y}\frac{\partial\delta w}{\partial x})-2M^b_{xy}\frac{\partial^2\delta w_b}{\partial x\partial y} \quad (13)$$
$$-2M^s_{xy}\frac{\partial^2\delta w_s}{\partial x\partial y}+Q_{yz}\frac{\partial\delta w_s}{\partial y}+Q_{xz}\frac{\partial\delta w_s}{\partial x}]dydx$$

in which

$$\begin{aligned}
N_{xx}&=\int_{-h/2}^{h/2}(\sigma^0_{xx}-\nabla\sigma^{(1)}_{xx})dz=N^{(0)}_{xx}-\nabla N^{(1)}_{xx}\\
N_{xy}&=\int_{-h/2}^{h/2}(\sigma^0_{xy}-\nabla\sigma^{(1)}_{xy})dz=N^{(0)}_{xy}-\nabla N^{(1)}_{xy}\\
N_{yy}&=\int_{-h/2}^{h/2}(\sigma^0_{yy}-\nabla\sigma^{(1)}_{yy})dz=N^{(0)}_{yy}-\nabla N^{(1)}_{yy}\\
M^b_{xx}&=\int_{-h/2}^{h/2}z(\sigma^0_{xx}-\nabla\sigma^{(1)}_{xx})dz=M^{b(0)}_{xx}-\nabla M^{b(1)}_{xx}\\
M^s_{xx}&=\int_{-h/2}^{h/2}f(\sigma^0_{xx}-\nabla\sigma^{(1)}_{xx})dz=M^{s(0)}_{xx}-\nabla M^{s(1)}_{xx}\\
M^b_{yy}&=\int_{-h/2}^{h/2}z(\sigma^0_{yy}-\nabla\sigma^{(1)}_{yy})dz=M^{b(0)}_{yy}-\nabla M^{b(1)}_{yy}\\
M^s_{yy}&=\int_{-h/2}^{h/2}f(\sigma^0_{yy}-\nabla\sigma^{(1)}_{yy})dz=M^{s(0)}_{yy}-\nabla M^{s(1)}_{yy}\\
M^b_{xy}&=\int_{-h/2}^{h/2}z(\sigma^0_{xy}-\nabla\sigma^{(1)}_{xy})dz=M^{b(0)}_{xy}-\nabla M^{b(1)}_{xy}\\
M^s_{xy}&=\int_{-h/2}^{h/2}f(\sigma^0_{xy}-\nabla\sigma^{(1)}_{xy})dz=M^{s(0)}_{xy}-\nabla M^{s(1)}_{xy}\\
Q_{xz}&=\int_{-h/2}^{h/2}g(\sigma^0_{xz}-\nabla\sigma^{(1)}_{xz})dz=Q^{(0)}_{xz}-\nabla Q^{(1)}_{xz}\\
Q_{yz}&=\int_{-h/2}^{h/2}g(\sigma^0_{yz}-\nabla\sigma^{(1)}_{yz})dz=Q^{(0)}_{yz}-\nabla Q^{(1)}_{yz}
\end{aligned} \quad (14a)$$

where

$$\begin{aligned}
N^{(0)}_{ij}&=\int_{-h/2}^{h/2}(\sigma^{(0)}_{ij})dz, \quad N^{(1)}_{ij}=\int_{-h/2}^{h/2}(\sigma^{(1)}_{ij})dz\\
M^{b(0)}_{ij}&=\int_{-h/2}^{h/2}z(\sigma^{b(0)}_{ij})dz, \quad M^{b(1)}_{ij}=\int_{-h/2}^{h/2}z(\sigma^{b(1)}_{ij})dz\\
M^{s(0)}_{ij}&=\int_{-h/2}^{h/2}f(\sigma^{s(0)}_{ij})dz, \quad M^{s(1)}_{ij}=\int_{-h/2}^{h/2}f(\sigma^{s(1)}_{ij})dz\\
Q^{(0)}_{xz}&=\int_{-h/2}^{h/2}g(\sigma^{i(0)}_{xz})dz, \quad Q^{(1)}_{xz}=\int_{-h/2}^{h/2}g(\sigma^{i(1)}_{xz})dz\\
Q^{(0)}_{yz}&=\int_{-h/2}^{h/2}g(\sigma^{i(0)}_{yz})dz, \quad Q^{(1)}_{yz}=\int_{-h/2}^{h/2}g(\sigma^{i(1)}_{yz})dz
\end{aligned} \quad (14b)$$

So that ($ij=xx$, xy, yy). The variation for the works of non-conservative force is expressed by

$$\begin{aligned}\delta V = \int_0^a\int_0^b (N_x^0 \frac{\partial(w_b+w_s)}{\partial x}\frac{\partial\delta(w_b+w_s)}{\partial x} + N_y^0 \frac{\partial(w_b+w_s)}{\partial y}\frac{\partial\delta(w_b+w_s)}{\partial y} \\ +2\delta N_{xy}^0 \frac{\partial(w_b+w_s)}{\partial x}\frac{\partial(w_b+w_s)}{\partial y} - k_w(w_b+w_s)\delta(w_b+w_s) - c_d\delta\frac{\partial(w_b+w_s)}{\partial t} \\ +k_p(\frac{\partial(w_b+w_s)}{\partial x}\frac{\partial\delta(w_b+w_s)}{\partial x} + \frac{\partial(w_b+w_s)}{\partial y}\frac{\partial\delta(w_b+w_s)}{\partial y}))dydx\end{aligned} \tag{15a}$$

where N_x^0, N_y^0, N_{xy}^0 denote membrane forces; k_w, k_p and c_d are viscoelastic substrate constants. Herein, the nano-dimension plate has been exposed to the below in-plane loading while shearing load has been neglected N_{xy}^0 =0

$$N_x^0 = N^T + N^H, \quad N_y^0 = N^T + N^H \tag{15b}$$

where hygro-thermal resultants may be defined as

$$\begin{aligned}N^T &= \int_{-h/2}^{h/2}\frac{E(z)}{1-v}\gamma(z)(T-T_0)\,dz \\ N^H &= \int_{-h/2}^{h/2}\frac{E(z)}{1-v}\beta(z)(C-C_0)\,dz\end{aligned} \tag{15c}$$

so that $C=\Delta C+C_0$ and $T=\Delta T+T_0$ define humidity and thermal variations; C_0 and T_0 express prescribed humidity and temperature.

Also, the kinetic energy variation is obtained as

$$\begin{aligned}\delta K = \int_0^a\int_0^b [I_0(\frac{\partial u}{\partial t}\frac{\partial\delta u}{\partial t} + \frac{\partial v}{\partial t}\frac{\partial\delta v}{\partial t} + \frac{\partial(w_b+w_s)}{\partial t}\frac{\partial\delta(w_b+w_s)}{\partial t}) - I_1(\frac{\partial u}{\partial t}\frac{\partial\delta w_b}{\partial x\partial t} + \frac{\partial w_b}{\partial x\partial t}\frac{\partial\delta u}{\partial t} + \frac{\partial v}{\partial t}\frac{\partial\delta w_b}{\partial y\partial t} \\ +\frac{\partial w_b}{\partial y\partial t}\frac{\partial\delta v}{\partial t}) - I_3(+\frac{\partial w_s}{\partial y\partial t}\frac{\partial\delta v}{\partial t} + \frac{\partial w_s}{\partial x\partial t}\frac{\partial\delta u}{\partial t} + \frac{\partial u}{\partial t}\frac{\partial\delta w_s}{\partial x\partial t} + \frac{\partial v}{\partial t}\frac{\partial\delta w_s}{\partial y\partial t}) + I_2(+\frac{\partial w_b}{\partial y\partial t}\frac{\partial\delta w_b}{\partial y\partial t} + \frac{\partial w_b}{\partial x\partial t}\frac{\partial\delta w_b}{\partial x\partial t}) \\ +I_5(+\frac{\partial w_s}{\partial y\partial t}\frac{\partial\delta w_s}{\partial y\partial t} + \frac{\partial w_s}{\partial x\partial t}\frac{\partial\delta w_s}{\partial x\partial t}) + I_4(\frac{\partial w_b}{\partial x\partial t}\frac{\partial\delta w_s}{\partial x\partial t} + \frac{\partial w_s}{\partial y\partial t}\frac{\partial\delta w_b}{\partial y\partial t} + \frac{\partial w_s}{\partial x\partial t}\frac{\partial\delta w_b}{\partial x\partial t} + \frac{\partial w_b}{\partial y\partial t}\frac{\partial\delta w_s}{\partial y\partial t})]dydx\end{aligned} \tag{16}$$

so that

$$(I_0, I_1, I_2, I_3, I_4, I_5) = \int_{-h/2}^{h/2}(1, z-r^*, (z-r^*)^2, \Upsilon-r^{**}, (z-r^*)(\Upsilon-r^{**}), (\Upsilon-r^{**})^2)\rho(z)dz \tag{17}$$

Substituting Eqs. (13)-(16) into Eq. (11) then collecting the coefficients for field variables results in four equations of motion

$$\frac{\partial N_x}{\partial x} + \frac{\partial N_{xy}}{\partial y} = I_0\frac{\partial^2 u}{\partial t^2} - I_1\frac{\partial^3 w_b}{\partial x\partial t^2} - I_3\frac{\partial^3 w_s}{\partial x\partial t^2} \tag{18}$$

$$\frac{\partial N_{xy}}{\partial x} + \frac{\partial N_y}{\partial y} = I_0\frac{\partial^2 v}{\partial t^2} - I_1\frac{\partial^3 w_b}{\partial y\partial t^2} - I_3\frac{\partial^3 w_s}{\partial y\partial t^2} \tag{19}$$

$$\begin{aligned}&\frac{\partial^2 M_x^b}{\partial x^2}+2\frac{\partial^2 M_{xy}^b}{\partial x\partial y}+\frac{\partial^2 M_y^b}{\partial y^2}-(N^T+N^H-k_p)[\frac{\partial^2(w_b+w_s)}{\partial x^2}+\frac{\partial^2(w_b+w_s)}{\partial y^2}]\\&-k_w(w_b+w_s)-c_d\frac{\partial(w_b+w_s)}{\partial t}=I_0\frac{\partial^2(w_b+w_s)}{\partial t^2}+I_1(\frac{\partial^3 u}{\partial x\partial t^2}+\frac{\partial^3 v}{\partial y\partial t^2})\\&-I_2(\frac{\partial^2}{\partial x^2}+\frac{\partial^2}{\partial y^2})(\frac{\partial^2 w_b}{\partial t^2})-I_4(\frac{\partial^2}{\partial x^2}+\frac{\partial^2}{\partial y^2})(\frac{\partial^2 w_s}{\partial t^2})\end{aligned}\tag{20}$$

$$\begin{aligned}&\frac{\partial^2 M_x^s}{\partial x^2}+2\frac{\partial^2 M_{xy}^s}{\partial x\partial y}+\frac{\partial^2 M_y^s}{\partial y^2}+\frac{\partial Q_{xz}}{\partial x}+\frac{\partial Q_{yz}}{\partial y}-(N^T+N^H-k_p)[\frac{\partial^2(w_b+w_s)}{\partial x^2}+\frac{\partial^2(w_b+w_s)}{\partial y^2}]\\&-k_w(w_b+w_s)-c_d\frac{\partial(w_b+w_s)}{\partial t}=I_0\frac{\partial^2(w_b+w_s)}{\partial t^2}\\&+I_3(\frac{\partial^3 u}{\partial x\partial t^2}+\frac{\partial^3 v}{\partial y\partial t^2})-I_4(\frac{\partial^2}{\partial x^2}+\frac{\partial^2}{\partial y^2})(\frac{\partial^2 w_b}{\partial t^2})-I_5(\frac{\partial^2}{\partial x^2}+\frac{\partial^2}{\partial y^2})(\frac{\partial^2 w_s}{\partial t^2})\end{aligned}\tag{21}$$

Next, all edge conditions for *x*=0, *a* and *y*=0, *b* may be expressed by

$$\begin{aligned}&\text{Specify } un_x+vn_y \text{ or } N_x n_x^2+2n_x n_y N_{xy}+N_y n_y^2=0\\&\text{Specify } -un_y+vn_x \text{ or } (N_y-N_x)n_x n_y+N_{xy}(n_x^2-n_y^2)=0\\&\text{Specify } w_b \text{ or } \left(\frac{\partial M_{xx}^b}{\partial x}+\frac{\partial M_{xy}^b}{\partial y}-I_1\frac{\partial^2 u}{\partial t^2}+I_2\frac{\partial^3 w_b}{\partial x\partial t^2}+I_4\frac{\partial^3 w_s}{\partial x\partial t^2}\right)n_x\\&\qquad+\left(\frac{\partial M_{yy}^b}{\partial y}+\frac{\partial M_{xy}^b}{\partial x}-I_1\frac{\partial^2 v}{\partial t^2}+I_2\frac{\partial^3 w_b}{\partial y\partial t^2}+I_4\frac{\partial^3 w_s}{\partial y\partial t^2}\right)n_y=0\\&\text{Specify } w_s \text{ or } \left(\frac{\partial M_{xx}^s}{\partial x}+\frac{\partial M_{xy}^s}{\partial y}+Q_{xz}-I_3\frac{\partial^2 u}{\partial t^2}+I_4\frac{\partial^3 w_b}{\partial x\partial t^2}+I_5\frac{\partial^3 w_s}{\partial x\partial t^2}\right)n_x\\&\qquad+\left(\frac{\partial M_{yy}^s}{\partial y}+\frac{\partial M_{xy}^s}{\partial x}+Q_{yz}-I_3\frac{\partial^2 v}{\partial t^2}+I_4\frac{\partial^3 w_b}{\partial y\partial t^2}+I_5\frac{\partial^3 w_s}{\partial y\partial t^2}\right)n_y=0\\&\text{Specify } \frac{\partial w_b}{\partial n} \text{ or } M_{xx}^b n_x^2+n_x n_y M_{xy}^b+M_{yy}^b n_y^2=0\end{aligned}\tag{22}$$

Note that ∂( )/∂*n*=n_x∂( )/∂*x*+n_y∂( )/∂*y*; n_x and n_y respectively define axial as well as lateral normal vectors at edges, and non-classic edge condition may be written as

$$\begin{aligned}&\text{Determine } \frac{\partial^2 w_b}{\partial x^2} \text{ or } M_{xx}^{b(1)}=0\\&\text{Determine } \frac{\partial^2 w_b}{\partial y^2} \text{ or } M_{yy}^{b(1)}=0\\&\text{Determine } \frac{\partial^2 w_s}{\partial x^2} \text{ or } M_{xx}^{s(1)}=0\\&\text{Determine } \frac{\partial^2 w_s}{\partial y^2} \text{ or } M_{yy}^{s(1)}=0\end{aligned}\tag{23}$$

Finally, the nonlocal strain gradient constitutive relations based on refined FG plate model can be expressed by

$$(1-\mu\nabla^2)\begin{Bmatrix}\sigma_x\\ \sigma_y\\ \sigma_{xy}\\ \sigma_{yz}\\ \sigma_{xz}\end{Bmatrix}=\frac{E(z)}{1-v^2}(1-\lambda\nabla^2)\begin{pmatrix}1 & v & 0 & 0 & 0\\ v & 1 & 0 & 0 & 0\\ 0 & 0 & (1-v)/2 & 0 & 0\\ 0 & 0 & 0 & (1-v)/2 & 0\\ 0 & 0 & 0 & 0 & (1-v)/2\end{pmatrix}\begin{Bmatrix}\varepsilon_x-\gamma\Delta T-\beta\Delta C\\ \varepsilon_y-\gamma\Delta T-\beta\Delta C\\ \gamma_{xy}\\ \gamma_{yz}\\ \gamma_{xz}\end{Bmatrix} \tag{24}$$

After integrating Eq. (24) in thickness direction, we get to the following relationships

$$(1-\mu\nabla^2)\begin{Bmatrix}N_x\\ N_y\\ N_{xy}\end{Bmatrix}=A(1-\lambda\nabla^2)\begin{pmatrix}1 & v & 0\\ v & 1 & 0\\ 0 & 0 & (1-v)/2\end{pmatrix}\begin{Bmatrix}\frac{\partial u}{\partial x}\\ \frac{\partial v}{\partial y}\\ \frac{\partial u}{\partial y}+\frac{\partial v}{\partial x}\end{Bmatrix} \tag{25}$$

$$(1-\mu\nabla^2)\begin{Bmatrix}M_x^b\\ M_y^b\\ M_{xy}^b\end{Bmatrix}=D(1-\lambda\nabla^2)\begin{pmatrix}1 & v & 0\\ v & 1 & 0\\ 0 & 0 & (1-v)/2\end{pmatrix}\begin{Bmatrix}-\frac{\partial^2 w_b}{\partial x^2}\\ -\frac{\partial^2 w_b}{\partial y^2}\\ -2\frac{\partial^2 w_b}{\partial x\partial y}\end{Bmatrix}+E(1-\lambda\nabla^2)\begin{pmatrix}1 & v & 0\\ v & 1 & 0\\ 0 & 0 & (1-v)/2\end{pmatrix}\begin{Bmatrix}-\frac{\partial^2 w_s}{\partial x^2}\\ -\frac{\partial^2 w_s}{\partial y^2}\\ -2\frac{\partial^2 w_s}{\partial x\partial y}\end{Bmatrix} \tag{26}$$

$$(1-\mu\nabla^2)\begin{Bmatrix}M_x^s\\ M_y^s\\ M_{xy}^s\end{Bmatrix}=E(1-\lambda\nabla^2)\begin{pmatrix}1 & v & 0\\ v & 1 & 0\\ 0 & 0 & (1-v)/2\end{pmatrix}\begin{Bmatrix}-\frac{\partial^2 w_b}{\partial x^2}\\ -\frac{\partial^2 w_b}{\partial y^2}\\ -2\frac{\partial^2 w_b}{\partial x\partial y}\end{Bmatrix}+F(1-\lambda\nabla^2)\begin{pmatrix}1 & v & 0\\ v & 1 & 0\\ 0 & 0 & (1-v)/2\end{pmatrix}\begin{Bmatrix}-\frac{\partial^2 w_s}{\partial x^2}\\ -\frac{\partial^2 w_s}{\partial y^2}\\ -2\frac{\partial^2 w_s}{\partial x\partial y}\end{Bmatrix} \tag{27}$$

$$(1-\mu\nabla^2)\begin{Bmatrix}Q_x\\ Q_y\end{Bmatrix}=A_{44}(1-\lambda\nabla^2)\begin{pmatrix}1 & 0\\ 0 & 1\end{pmatrix}\begin{Bmatrix}\frac{\partial w_s}{\partial x}\\ \frac{\partial w_s}{\partial y}\end{Bmatrix} \tag{28}$$

in which

$$\begin{aligned}&A=\int_{-h/2}^{h/2}\frac{E(z)}{1-v^2}dz,\ \ D=\int_{-h/2}^{h/2}\frac{E(z)(z-r^*)^2}{1-v^2}dz,\ \ E=\int_{-h/2}^{h/2}\frac{E(z)(z-r^*)(\Upsilon-r^{**})}{1-v^2}dz\\ &F=\int_{-h/2}^{h/2}\frac{E(z)(\Upsilon-r^{**})^2}{1-v^2}dz,\quad A_{44}=\int_{-h/2}^{h/2}\frac{E(z)}{2(1+v)}g^2dz\end{aligned} \tag{29}$$

Three equations of motion based on neutral surface location will be achieved by placing Eqs.

(25)-(28) in Eqs. (18)-(21) by

$$A(1-\lambda\nabla^2)(\frac{\partial^2 u}{\partial x^2}+\frac{1-\nu}{2}\frac{\partial^2 u}{\partial y^2}+\frac{1+\nu}{2}\frac{\partial^2 v}{\partial x\partial y})+(1-\mu\nabla^2)(-I_0\frac{\partial^2 u}{\partial t^2}+I_1\frac{\partial^3 w_b}{\partial x\partial t^2}+I_3\frac{\partial^3 w_s}{\partial x\partial t^2})=0 \tag{30}$$

$$A(1-\lambda\nabla^2)(\frac{\partial^2 v}{\partial y^2}+\frac{1-\nu}{2}\frac{\partial^2 v}{\partial x^2}+\frac{1+\nu}{2}\frac{\partial^2 u}{\partial x\partial y})+(1-\mu\nabla^2)(-I_0\frac{\partial^2 v}{\partial t^2}+I_1\frac{\partial^3 w_b}{\partial y\partial t^2}+I_3\frac{\partial^3 w_s}{\partial y\partial t^2})=0 \tag{31}$$

$$\begin{aligned}&-D(1-\lambda\nabla^2)(\frac{\partial^4 w_b}{\partial x^4}+2\frac{\partial^4 w_b}{\partial x^2\partial y^2}+\frac{\partial^4 w_b}{\partial y^4})-E(1-\lambda\nabla^2)(\frac{\partial^4 w_s}{\partial x^4}+2\frac{\partial^4 w_s}{\partial x^2\partial y^2}+\frac{\partial^4 w_s}{\partial y^4})\\&+(1-\mu\nabla^2)(-I_0\frac{\partial^2(w_b+w_s)}{\partial t^2}-I_1(\frac{\partial^3 u}{\partial x\partial t^2}+\frac{\partial^3 v}{\partial y\partial t^2})+I_2\nabla^2(\frac{\partial^2 w_b}{\partial t^2})\\&+I_4\nabla^2(\frac{\partial^2 w_s}{\partial t^2})-(N^T+N^H)[\frac{\partial^2(w_b+w_s)}{\partial x^2}+\frac{\partial^2(w_b+w_s)}{\partial y^2}]\\&-(k_w+\frac{\partial}{\partial t}c_d)(w_b+w_s)+k_P[\frac{\partial^2(w_b+w_s)}{\partial x^2}+\frac{\partial^2(w_b+w_s)}{\partial y^2}])=0\end{aligned} \tag{32}$$

$$\begin{aligned}&-E(1-\lambda\nabla^2)(\frac{\partial^4 w_b}{\partial x^4}+2\frac{\partial^4 w_b}{\partial x^2\partial y^2}+\frac{\partial^4 w_b}{\partial y^4})-F(1-\lambda\nabla^2)(\frac{\partial^4 w_s}{\partial x^4}+2\frac{\partial^4 w_s}{\partial x^2\partial y^2}+\frac{\partial^4 w_s}{\partial y^4})\\&+A_{44}(1-\lambda\nabla^2)(\frac{\partial^2 w_s}{\partial x^2}+\frac{\partial^2 w_s}{\partial y^2})+(1-\mu\nabla^2)(-I_0\frac{\partial^2(w_b+w_s)}{\partial t^2}-I_3(\frac{\partial^3 u}{\partial x\partial t^2}+\frac{\partial^3 v}{\partial y\partial t^2})\\&+I_4\nabla^2(\frac{\partial^2 w_b}{\partial t^2})+I_5\nabla^2(\frac{\partial^2 w_s}{\partial t^2})-(N^T+N^H)[\frac{\partial^2(w_b+w_s)}{\partial x^2}+\frac{\partial^2(w_b+w_s)}{\partial y^2}]\\&-(k_w+\frac{\partial}{\partial t}c_d)(w_b+w_s)+k_p[\frac{\partial^2(w_b+w_s)}{\partial x^2}+\frac{\partial^2(w_b+w_s)}{\partial y^2}])=0\end{aligned} \tag{33}$$

4. Solution by differential quadrature method (DQM)

In the present chapter, differential quadrature method (DQM) has been utilized for solving the governing equations for NSGT porous FG nanoplate. According to DQM, at an assumed grid point (x_i, y_j) the derivatives for function F are supposed as weighted linear summation of all functional values within the computation domains as

$$\frac{d^nF}{dx^n}\Big|_{x=x_i}=\sum_{j=1}^{N} c_{ij}^{(n)}F(x_j) \tag{34}$$

where

$$C_{ij}^{(1)}=\frac{\pi(x_i)}{(x_i-x_j)\,\pi(x_j)} \qquad i,j=1,2,\dots,N, \qquad i\neq j \tag{35}$$

in which $\pi(x_i)$ is defined by

$$\pi(x_i)=\prod_{j=1}^{N}(x_i-x_j), \quad i\neq j \tag{36}$$

And when $i=j$

$$C_{ij}^{(1)} = c_{ii}^{(1)} = -\sum_{k=1}^{N} C_{ik}^{(1)}, \quad i = 1,2,\dots,N, \quad i \neq k,\ i = j \tag{37}$$

Then, weighting coefficients for high orders derivatives may be expressed by

$$\begin{gathered} C_{ij}^{(2)} = \sum_{k=1}^{N} C_{ik}^{(1)} C_{kj}^{(1)} \\ C_{ij}^{(3)} = \sum_{k=1}^{N} C_{ik}^{(1)} C_{kj}^{(2)} = \sum_{k=1}^{N} C_{ik}^{(2)} C_{kj}^{(1)} \\ C_{ij}^{(4)} = \sum_{k=1}^{N} C_{ik}^{(1)} C_{kj}^{(3)} = \sum_{k=1}^{N} C_{ik}^{(3)} C_{kj}^{(1)} \qquad i,j = 1,2,\dots,N. \\ C_{ij}^{(5)} = \sum_{k=1}^{N} C_{ik}^{(1)} C_{kj}^{(4)} = \sum_{k=1}^{N} C_{ik}^{(4)} C_{kj}^{(1)} \\ C_{ij}^{(6)} = \sum_{k=1}^{N} C_{ik}^{(1)} C_{kj}^{(5)} = \sum_{k=1}^{N} C_{ik}^{(5)} C_{kj}^{(1)} \end{gathered} \tag{38}$$

According to presented approach, the dispersions of grid points based upon Gauss-Chebyshev-Lobatto assumption are expressed as

$$\begin{aligned} x_i &= \frac{a}{2}\left[1 - \cos\left(\frac{i-1}{N-1}\pi\right)\right] \qquad i = 1,2,\dots,N, \\ y_j &= \frac{b}{2}\left[1 - \cos\left(\frac{j-1}{M-1}\pi\right)\right] \qquad j = 1,2,\dots,M, \end{aligned} \tag{39}$$

Next, the time derivative for displacement components may be determined by

$$w_b(x,y,t) = W_b(x,y)e^{i\omega t} \tag{40}$$

$$w_s(x,y,t) = W_s(x,y)e^{i\omega t} \tag{41}$$

where W_b and W_n denote vibration amplitudes and ω defines the vibrational frequency. Then, it is possible to express obtained boundary conditions as

$$\begin{aligned} & w_b = w_s = 0, \\ & \frac{\partial^2 w_b}{\partial x^2} = \frac{\partial^2 w_s}{\partial x^2} = \frac{\partial^2 w_b}{\partial y^2} = \frac{\partial^2 w_s}{\partial y^2} = 0 \\ & \frac{\partial^4 w_b}{\partial x^4} = \frac{\partial^4 w_s}{\partial x^4} = \frac{\partial^4 w_b}{\partial y^4} = \frac{\partial^4 w_s}{\partial y^4} = 0 \end{aligned} \tag{42}$$

Now, one can express the modified weighting coefficients for all edges simply-supported as

$$\begin{aligned} \bar{C}_{1,j}^{(2)} = \bar{C}_{N,j}^{(2)} = 0, \qquad i = 1,2,\dots,M, \\ \bar{C}_{i,1}^{(2)} = \bar{C}_{1,M}^{(2)} = 0, \qquad i = 1,2,\dots,N. \end{aligned} \tag{43}$$

and

$$\bar{C}_{ij}^{(3)} = \sum_{k=1}^{N} C_{ik}^{(1)} \bar{C}_{kj}^{(2)} \qquad \bar{C}_{ij}^{(4)} = \sum_{k=1}^{N} C_{ik}^{(1)} \bar{C}_{kj}^{(3)} \tag{44}$$

By placing Eqs. (38)-(39) into Eqs. (30)-(33) and performing some simplifications leads to the following system based on mass matrix [M], stiffness matrix [K] and damping matrix [C] as

$$\left\{[K] + i\bar{\omega}_n[C] + \bar{\omega}_n{}^2[M]\right\} \begin{Bmatrix} U_{mn} \\ V_{mn} \\ W_{bmn} \\ W_{smn} \end{Bmatrix} = 0 \tag{45}$$

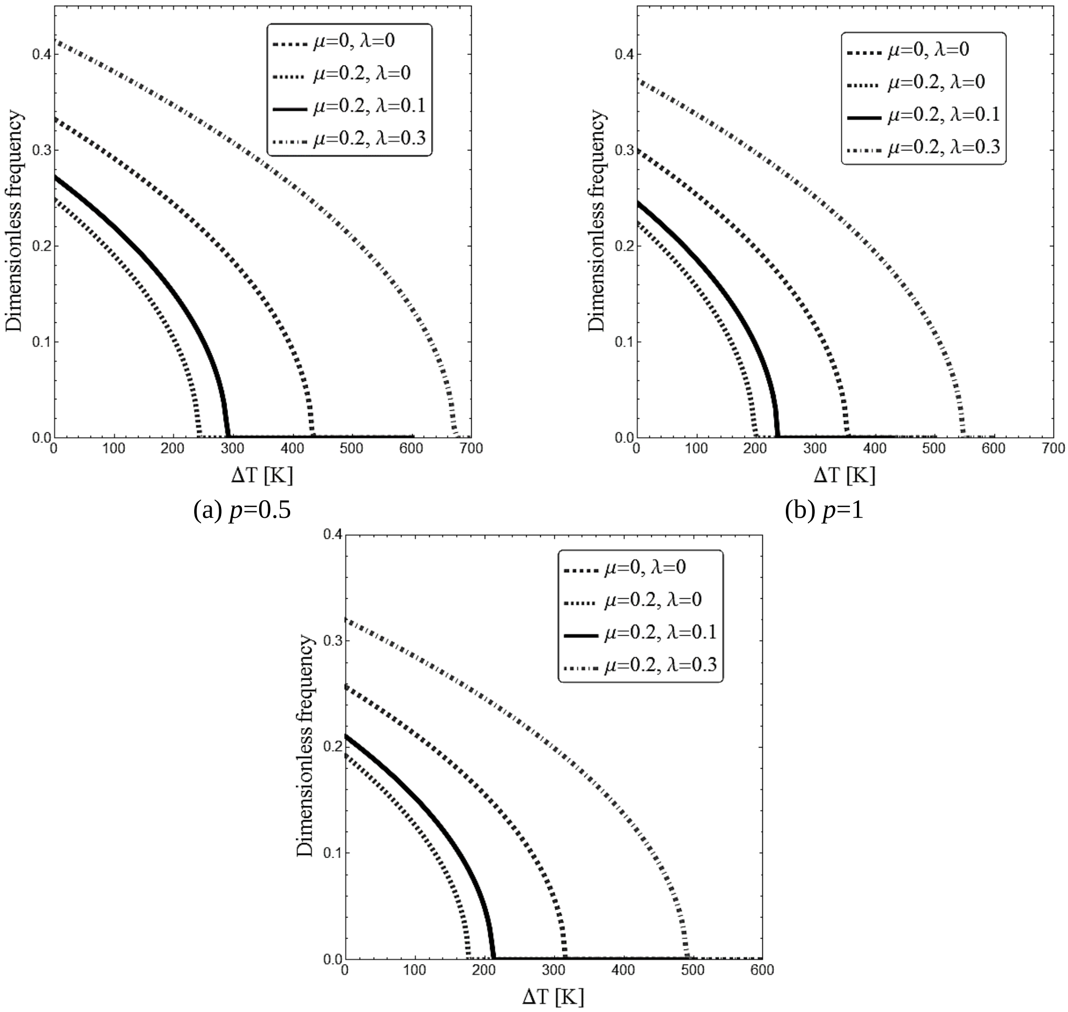

(a) p=0.5 (b) p=1

(c) p=5

Fig. 2 Changing of normalized frequency for ideal nanoplates with respect to temperature variation based on diverse nonlocality and strain gradients factors (a/h=15, K_w=0, K_p=0, ΔC=0%)

Six grid points are adequate for convergence of the method. The presented results are based on the following dimensionless factors

$$\hat{\omega}=\omega a\sqrt{\frac{\rho_c}{\mathrm{E}_c}}\,,\ K_w=\frac{k_w a^4}{D_c},K_p=\frac{k_p a^2}{D_c},C_d=c_d\,\frac{a^2}{\sqrt{\rho h D_c}},D_c=\frac{E_c h^3}{12(1-v_c^2)} \tag{46}$$

5. Obtained results and discussions

This section studies vibrational behaviors of porous FG nano-dimension plates coupled by visco-elastic foundation using secant function based four-variable plate model and DQ approach. Nonlocal

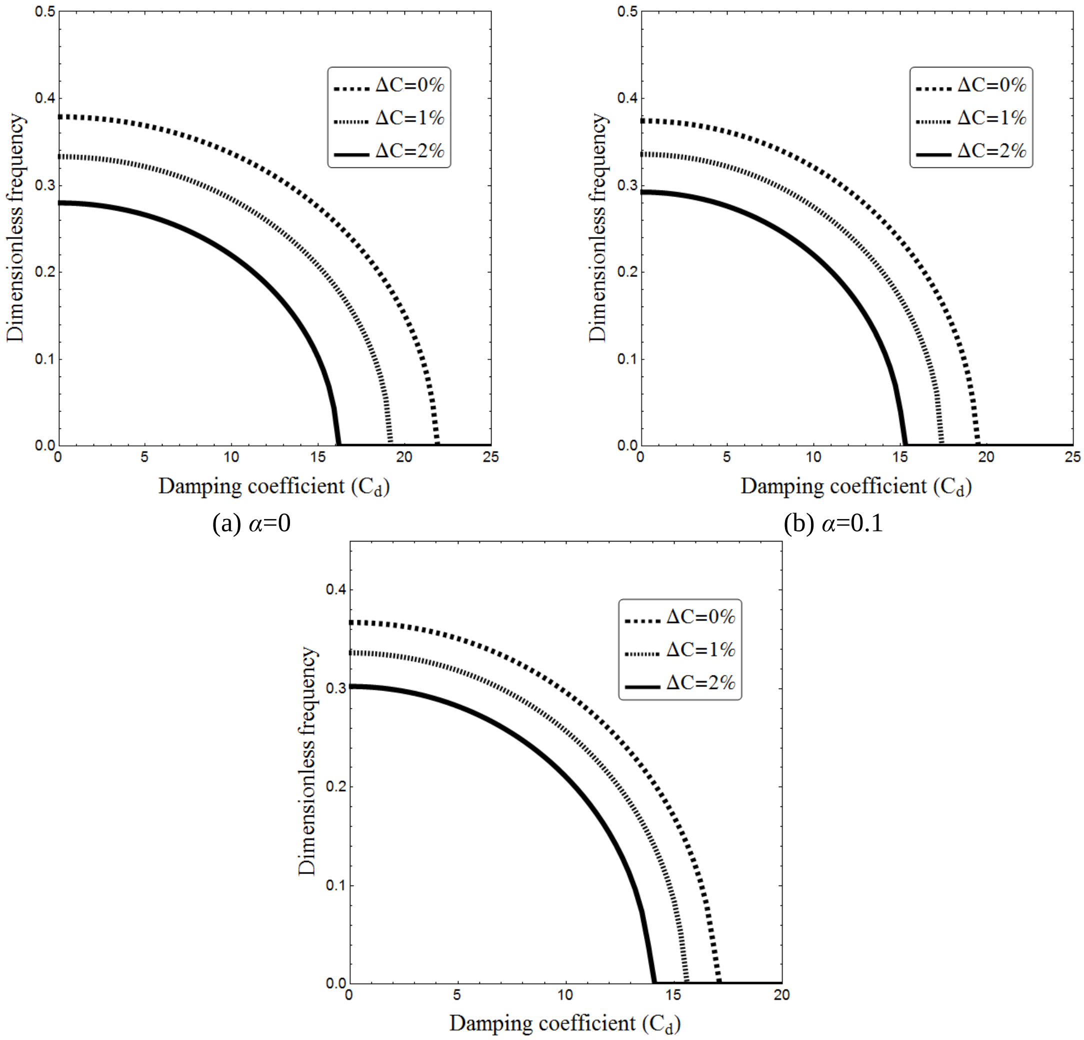

(a) α=0 (b) α=0.1

(c) α=0.2

Fig. 3 Normalized frequency of FG nanoplate according to damping coefficient for diverse pore volume fraction (p=1, a/h=10, ΔT=10, K_w=5, K_p=0.5, μ=0.2, λ=0.1)

and strain gradient coefficients are used in order to define the size-dependent behavior of nano-size plate. Presented results indicate the prominence of moisture/temperature variation, damping factor, material gradient index, nonlocal coefficient, strain gradient coefficient and porosities on vibrational frequencies of FG nano-size plate. A verification study is presented in Table 1 for FG nanoplate with comparing the vibrational frequency presented by DQM and those obtained by Natarajan *et al*. 2012. Also, each material property for FG plate may be assumed by:

- $E_c = 380 \ GPa, \ \rho_c = 3800 \, kg/m^3$, $\nu_c = 0.3$, $\gamma_c = 7 \times 10^{-6} \, 1/\,^0C$, $\beta_c = 0.001 \, (wt.\% \, H_2o)^{-1}$
- $E_m = 70 \ GPa, \ \rho_m = 2707 \, kg/m^3$, $\nu_m = 0.3$, $\gamma_m = 23 \times 10^{-6} \, 1/\,^0C$, $\beta_m = 0.44 \, (wt.\% \, H_2o)^{-1}$

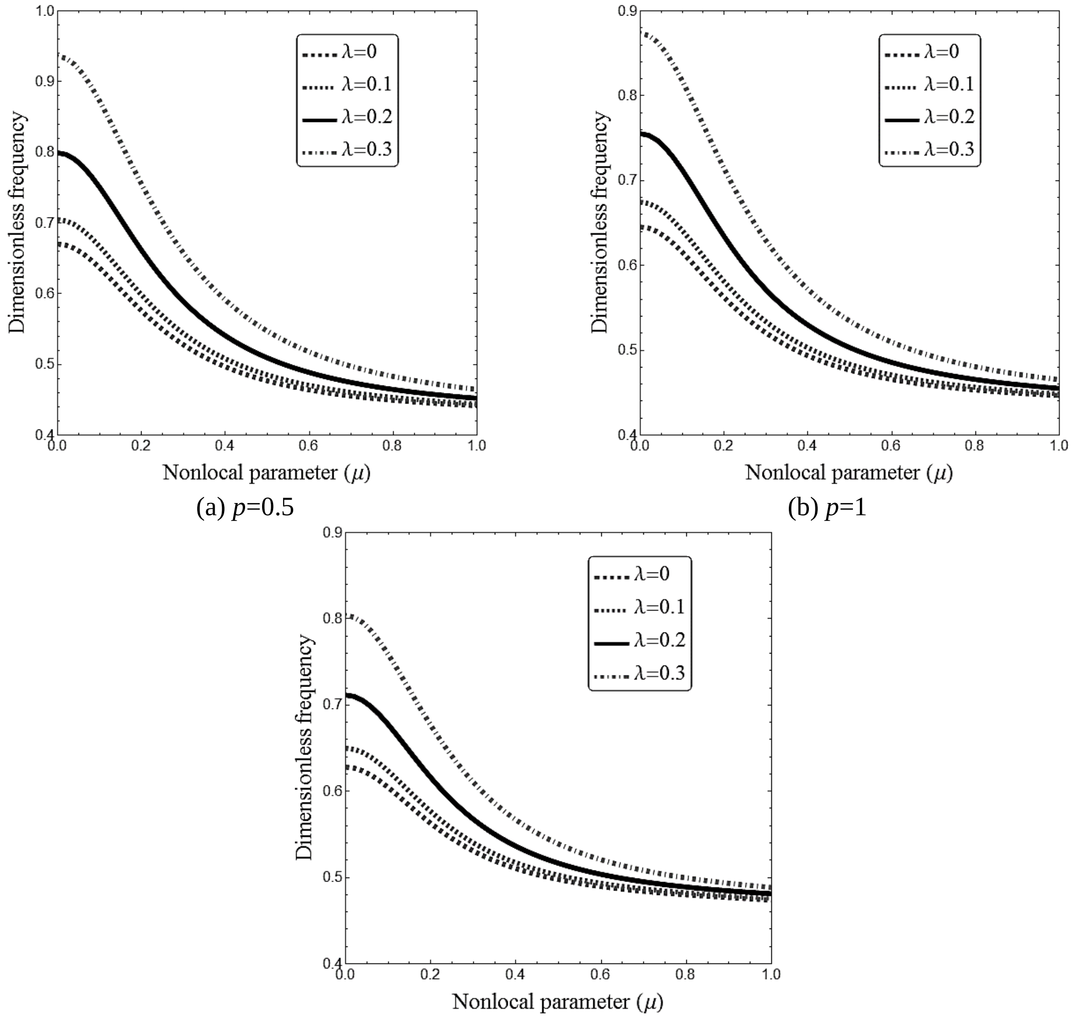

(a) p=0.5 (b) p=1 (c) p=5

Fig. 4 Changing of normalized frequency of porous nanoplates according to nonlocal coefficient based on diverse strain gradients coefficient (ΔT=50, ΔC=1%, a/h=10, K_w=25, K_p=10)

In Fig. 2, one can see the variation of vibrational frequency versus temperature for a variety of both nonlocal and strain gradient coefficients. This figure has three parts and each part is related to one value for material gradient index. Porosity parameter for nanoplates is chosen to be zero. It can be understand from Fig. 2 that vibration frequency of system will rise with strain gradient coefficient and will reduce with nonlocality coefficient. This observation is valid for all values of material gradient index. So, vibration behavior of double nanoplate system is dependent on both scale effects.

In Fig. 3 one can see the variation of vibrational frequency of nanoplate system versus damping factor of visco-elastic substrate with different porosity coefficients. Thus, the effect of surrounding visco-medium is considered for this figure. It can be understand from Fig. 3 that vibration frequency of system will reduce with pore coefficient and humidity rise. By considering visco-elastic substrate, vibrational frequency will reduce with the damping factor magnitude. So, the nanoplate system will be less rigid as the damping factor or visco-elastic parameters become stiffer.

One can see from Fig. 4 the variation of vibrational frequency of the nano-size plate against non-local and strain gradient coefficients when a=10h. Void or pore dispersion is set as uniform with different values for material gradient index (p). The vibration frequency of a large-size plate might be achieved by selecting a zero non-local parameter. From the figure, it might be seen that non-local coefficient assigns a stiffness devaluation characteristic together with a smaller vibration frequency. Besides, growth of material gradient index yields a smaller frequency regardless of non-local parameter magnitude.

6. Conclusions

This article focused on vibration characteristic of a nanoplate system coupled by visco-elastic medium and modeled by NSGT and refined plate theories. Nanoplates were considered to be porosity-dependent accounting for thermal effects. It was understood that vibration frequency of system raised with strain gradient coefficient and reduced with nonlocality coefficient. It was also found that vibration frequency of system might reduce with pore coefficient. By considering visco-elastic substrate, vibrational frequency will reduce with the damping factor magnitude. Besides, growth of material gradient index yields a smaller frequency regardless of non-local parameter magnitude.

Acknowledgement

The authors would like to thank Mustansiriyah university (www.uomustansiriyah.edu.iq) Baghdad-Iraq for its support in the present work.

References

Aissani, K., Bouiadjra, M.B., Ahouel, M. and Tounsi, A. (2015), "A new nonlocal hyperbolic shear deformation theory for nanobeams embedded in an elastic medium", *Struct. Eng. Mech.*, **55**(4), 743-763. https://doi.org/10.12989/sem.2015.55.4.743.

Alasadi, A.A., Ahmed, R.A. and Faleh, N.M. (2019), "Analyzing nonlinear vibrations of metal foam nanobeams with symmetric and non-symmetric porosities", *Adv. Aircraft Spacecraft Sci.*, **6**(4), 273. https://doi.org/10.12989/aas.2019.6.4.273.

Atmane, H.A., Tounsi, A. and Bernard, F. (2017), "Effect of thickness stretching and porosity on mechanical response of a functionally graded beams resting on elastic foundations", *Int. J. Mech. Mater. Des.*, **13**(1), 71-84. https://doi.org/10.1007/s10999-015-9318-x.

Attia, A., Bousahla, A.A., Tounsi, A., Mahmoud, S.R. and Alwabli, A.S. (2018), "A refined four variable plate theory for thermoelastic analysis of FGM plates resting on variable elastic foundations", *Struct. Eng. Mech.*, **65**(4), 453-464. https://doi.org/10.12989/sem.2018.65.4.453.

Barati, M.R. and Zenkour, A. (2017), "A general bi-Helmholtz nonlocal strain-gradient elasticity for wave propagation in nanoporous graded double-nanobeam systems on elastic substrate", *Compos. Struct.*, **168**, 885-892. https://doi.org/10.1016/j.compstruct.2017.02.090.

Belkorissat, I., Houari, M.S.A., Tounsi, A., Bedia, E.A. and Mahmoud, S.R. (2015), "On vibration properties of functionally graded nano-plate using a new nonlocal refined four variable model", *Steel Compos. Struct.*, **18**(4), 1063-1081. http://dx.doi.org/10.12989/scs.2015.18.4.1063.

Berghouti, H., Bedia, E.A., Benkhedda, A. and Tounsi, A. (2019), "Vibration analysis of nonlocal porous nanobeams made of functionally graded material", *Adv. Nano Res.*, **7**(5), 351-364. https://doi.org/10.12989/anr.2019.7.5.351.
Berrabah, H.M., Tounsi, A., Semmah, A. and Adda, B. (2013), "Comparison of various refined nonlocal beam theories for bending, vibration and buckling analysis of nanobeams", *Struct. Eng. Mech.*, **48**(3), 351-365. https://doi.org/10.12989/sem.2013.48.3.351.
Besseghier, A., Heireche, H., Bousahla, A.A., Tounsi, A. and Benzair, A. (2015), "Nonlinear vibration properties of a zigzag single-walled carbon nanotube embedded in a polymer matrix", *Adv. Nano Res.*, **3**(1), 029. https://doi.org/10.12989/anr.2015.3.1.029.
Besseghier, A., Houari, M.S.A., Tounsi, A. and Mahmoud, S.R. (2017), "Free vibration analysis of embedded nanosize FG plates using a new nonlocal trigonometric shear deformation theory", *Smart Struct. Syst.*, **19**(6), 601-614. https://doi.org/10.12989/sss.2017.19.6.601.
Bouadi, A., Bousahla, A.A., Houari, M.S.A., Heireche, H and Tounsi, A. (2018), "A new nonlocal HSDT for analysis of stability of single layer graphene sheet", *Adv. Nano Res.*, **6**(2), 147-162. https://doi.org/10.12989/anr.2018.6.2.147.
Bouafia, K., Kaci, A., Houari, M.S.A., Benzair, A and Tounsi, A. (2017), "A nonlocal quasi-3D theory for bending and free flexural vibration behaviors of functionally graded nanobeams", *Smart Struct. Syst.*, **19**(2), 115-126. https://doi.org/10.12989/sss.2017.19.2.115.
Bouderba, B., Houari, M.S.A., Tounsi, A. and Mahmoud, S.R. (2016), "Thermal stability of functionally graded sandwich plates using a simple shear deformation theory", *Struct. Eng. Mech.*, **58**(3), 397-422. https://doi.org/10.12989/sem.2016.58.3.397.
Boulefrakh, L., Hebali, H., Chikh, A., Bousahla, A.A., Tounsi, A. and Mahmoud, S.R. (2019), "The effect of parameters of visco-Pasternak foundation on the bending and vibration properties of a thick FG plate", *Geomech. Eng.*, **18**(2), 161-178. https://doi.org/10.12989/gae.2019.18.2.161.
Bourada, M., Kaci, A., Houari, M.S.A. and Tounsi, A. (2015), "A new simple shear and normal deformations theory for functionally graded beams", *Steel Compos. Struct.*, **18**(2), 409-423. https://doi.org/10.12989/scs.2015.18.2.409.
Chaabane, L.A., Bourada, F., Sekkal, M., Zerouati, S., Zaoui, F.Z., Tounsi, A., ... & Tounsi, A. (2019), "Analytical study of bending and free vibration responses of functionally graded beams resting on elastic foundation", *Struct. Eng. Mech.*, **71**(2), 185-196. https://doi.org/10.12989/sem.2019.71.2.185.
Chikh, A., Bakora, A., Heireche, H., Houari, M.S.A., Tounsi, A. and Bedia, E.A. (2016), "Thermo-mechanical postbuckling of symmetric S-FGM plates resting on Pasternak elastic foundations using hyperbolic shear deformation theory", *Struct. Eng. Mech.*, **57**(4), 617-639. https://doi.org/10.12989/sem.2016.57.4.617
Daneshmehr, A. and Rajabpoor, A. (2014), "Stability of size dependent functionally graded nanoplate based on nonlocal elasticity and higher order plate theories and different boundary conditions", *Int. J. Eng. Sci.*, **82**, 84-100. https://doi.org/10.1016/j.ijengsci.2014.04.017.
Daouadji, T.H., Benferhat, R and Adim, B. (2016), "A novel higher order shear deformation theory based on the neutral surface concept of FGM plate under transverse load", *Adv. Mater. Res.*, **5**(2), 107-120. https://doi.org/10.12989/amr.2016.5.2.107.
Draiche, K., Tounsi, A. and Mahmoud, S.R. (2016), "A refined theory with stretching effect for the flexure analysis of laminated composite plates", *Geomech. Eng.*, **11**(5), 671-690. https://doi.org/10.12989/gae.2016.11.5.671.
El-Hassar, S.M., Benyoucef, S., Heireche, H. and Tounsi, A. (2016), "Thermal stability analysis of solar functionally graded plates on elastic foundation using an efficient hyperbolic shear deformation theory", *Geomech. Eng.*, **10**(3), 357-386. https://doi.org/10.12989/gae.2016.10.3.357.
Elmerabet, A.H., Heireche, H., Tounsi, A. and Semmah, A. (2017), "Buckling temperature of a single-walled boron nitride nanotubes using a novel nonlocal beam model", *Adv. Nano Res.*, **5**(1), 1-12. https://doi.org/10.12989/anr.2017.5.1.001.
Eringen, A.C. (1983), "On differential equations of nonlocal elasticity and solutions of screw dislocation and surface waves", *J. Appl. Phys.*, **54**(9), 4703-4710. https://doi.org/10.1063/1.332803.
Faleh, N.M., Fenjan, R.M. and Ahmed, R.A. (2018), "Dynamic analysis of graded small-scale shells with

porosity distributions under transverse dynamic loads", *Eur. Phys. J. Plus*, **133**(9), 348. https://doi.org/10.1140/epjp/i2018-12152-5.

Fenjan, R.M., Ahmed, R.A., Alasadi, A.A. and Faleh, N.M. (2019), "Nonlocal strain gradient thermal vibration analysis of double-coupled metal foam plate system with uniform and non-uniform porosities", *Coupl. Syst. Mech.*, **8**(3), 247-257. https://doi.org/10.12989/csm.2019.8.3.247.

Houari, M.S.A., Tounsi, A., Bessaim, A. and Mahmoud, S.R. (2016), "A new simple three-unknown sinusoidal shear deformation theory for functionally graded plates", *Steel Compos. Struct.*, **22**(2), 257-276. https://doi.org/10.12989/scs.2016.22.2.257.

Issad, M.N., Fekrar, A., Bakora, A., Bessaim, A. and Tounsi, A. (2018), "Free vibration and buckling analysis of orthotropic plates using a new two variable refined plate theory", *Geomech. Eng.*, **15**(1), 711-719. https://doi.org/10.12989/gae.2018.15.1.711.

Jabbari, M., Vaghari, A.R., Bahtui, A. and Eslami, M.R. (2008), "Exact solution for asymmetric transient thermal and mechanical stresses in FGM hollow cylinders with heat source", *Struct. Eng. Mech.*, **29**(5), 551-565. https://doi.org/10.12989/sem.2008.29.5.551.

Karami, B., Janghorban, M. and Tounsi, A (2018b), "Nonlocal strain gradient 3D elasticity theory for anisotropic spherical nanoparticles", *Steel Compos. Struct.*, **27**(2), 201-216. https://doi.org/10.12989/scs.2018.27.2.201.

Karami, B., Janghorban, M. and Tounsi, A (2019a), "On pre stressed functionally graded anisotropic nanoshell in magnetic feld", *J. Brazil. Soc. Mech. Sci. Eng.*, **41**(11), 495. https://doi.org/10.1007/s40430-019-1996-0.

Karami, B., Janghorban, M. and Tounsi, A. (2019b), "Wave propagation of functionally graded anisotropic nanoplates resting on Winkler-Pasternak foundation", *Struct. Eng. Mech.*, **7**(1), 55-66. https://doi.org/10.12989/sem.2019.70.1.055.

Karami, B., Janghorban, M. and Tounsi, A. (2019c), "On exact wave propagation analysis of triclinic material using three dimensional bi-Helmholtz gradient plate model", *Struct. Eng. Mech.*, **69**(5), 487-497. https://doi.org/10.12989/sem.2019.69.5.487.

Karami, B., Janghorban, M. and Tounsi, A. (2019d), "Wave propagation of functionally graded anisotropic nanoplates resting on Winkler-Pasternak foundation", *Struct. Eng. Mech.*, **7**(1), 55-66. https://doi.org/10.12989/sem.2019.70.1.055.

Karami, B., Janghorban, M., Shahsavari, D. and Tounsi, A. (2018a), "A size-dependent quasi-3D model for wave dispersion analysis of FG nanoplates", *Steel Compos. Struct.*, **28**(1), 99-110. https://doi.org/10.12989/scs.2018.28.1.099.

Khiloun, M., Bousahla, A.A., Kaci, A., Bessaim, A., Tounsi, A. and Mahmoud, S.R. (2019), "Analytical modeling of bending and vibration of thick advanced composite plates using a four-variable quasi 3D HSDT", Engineering with Computers., **36**, 807-821. https://doi.org/10.1007/s00366-019-00732-1.

Lal, A., Jagtap, K.R and Singh, B.N. (2017), "Thermo-mechanically induced finite element based nonlinear static response of elastically supported functionally graded plate with random system properties", *Adv. Comput. Des.*, **2**(3), 165-194. https://doi.org/10.12989/acd.2017.2.3.165.

Lam, D.C., Yang, F., Chong, A.C.M., Wang, J. and Tong, P. (2003), "Experiments and theory in strain gradient elasticity", *J. Mech. Phys. Solid.*, **51**(8), 1477-1508. https://doi.org/10.1016/S0022-5096(03)00053-X.

Larbi Chaht, F., Kaci, A., Houari, M.S.A., Tounsi, A., Anwar Bég, O. and Mahmoud, S.R. (2015), "Bending and buckling analyses of functionally graded material (FGM) size-dependent nanoscale beams including the thickness stretching effect", *Steel Compos. Struct.*, **18**(2), 425-442. https://doi.org/10.12989/scs.2015.18.2.425.

Lim, C.W., Zhang, G. and Reddy, J.N. (2015), "A higher-order nonlocal elasticity and strain gradient theory and its applications in wave propagation", *J. Mech. Phys. Solid.*, **78**, 298-313. https://doi.org/10.1016/j.jmps.2015.02.001.

Mahi, A., Adda Bedia, E.A. and Tounsi, A. (2015), "A new hyperbolic shear deformation theory for bending and free vibration analysis of isotropic, functionally graded, sandwich and laminated composite plates", *Appl. Math. Model.*, **39**, 2489-2508. https://doi.org/10.1016/j.apm.2014.10.045.

Mahmoudi, A., Benyoucef, S., Tounsi, A., Benachour, A., Adda Bedia, E.A. and Mahmoud, S.R. (2019), "A refined quasi-3D shear deformation theory for thermo-mechanical behavior of functionally graded sandwich plates on elastic foundations", *J. Sandw. Struct. Mater.*, **21**(6), 1906-1929. https://doi.org/10.1177/1099636217727577.

Medani, M., Benahmed, A., Zidour, M., Heireche, H., Tounsi, A., Bousahla, A.A. and Mahmoud, S.R. (2019), "Static and dynamic behavior of (FG-CNT) reinforced porous sandwich plate using energy principle", *Steel Compos. Struct.*, **32**(5), 595-610. https://doi.org/10.12989/scs.2019.32.5.595.

Meksi, R., Benyoucef, S., Mahmoudi, A., Tounsi, A., Adda Bedia, E.A. and Mahmoud, S.R. (2019), "An analytical solution for bending, buckling and vibration responses of FGM sandwich plates", *J. Sandw. Struct. Mater.*, **21**(2), 727-757. https://doi.org/10.1177/1099636217698443.

Merazi, M., Hadji, L., Daouadji, T.H., Tounsi, A. and Adda Bedia, E.A. (2015), "A new hyperbolic shear deformation plate theory for static analysis of FGM plate based on neutral surface position", *Geomech. Eng.*, **8**(3), 305-321. https://doi.org/10.12989/gae.2015.8.3.305.

Mirsalehi, M., Azhari, M. and Amoushahi, H. (2017), "Buckling and free vibration of the FGM thin micro-plate based on the modified strain gradient theory and the spline finite strip method", *Eur. J. Mech.-A/Solid.*, **61**, 1-13. https://doi.org/10.1016/j.euromechsol.2016.08.008.

Natarajan, S., Chakraborty, S., Thangavel, M., Bordas, S. and Rabczuk, T. (2012), "Size-dependent free flexural vibration behavior of functionally graded nanoplates", *Comput. Mater. Sci.*, **65**, 74-80. https://doi.org/10.1016/j.commatsci.2012.06.031.

Sadoun, M., Houari, M.S.A., Bakora, A., Tounsi, A., Mahmoud, S.R. and Alwabli, A.S. (2018), "Vibration analysis of thick orthotropic plates using quasi 3D sinusoidal shear deformation theory", *Geomech. Eng.*, **16**(2), 141-150. https://doi.org/10.12989/gae.2018.16.2.141.

Sayyad, A.S. and Ghugal, Y.M. (2018), "An inverse hyperbolic theory for FG beams resting on Winkler-Pasternak elastic foundation", *Adv. Aircraft Spacecraft Sci.*, **5**(6), 671-689. https://doi.org/10.12989/aas.2018.5.6.671.

Sedighi, H.M., Daneshmand, F. and Abadyan, M. (2015), "Modified model for instability analysis of symmetric FGM double-sided nano-bridge: corrections due to surface layer, finite conductivity and size effect", *Compos. Struct.*, **132**, 545-557. https://doi.org/10.1016/j.compstruct.2015.05.076.

Semmah, A., Heireche, H., Bousahla, A.A. and Tounsi, A. (2019), "Thermal buckling analysis of SWBNNT on Winkler foundation by non local FSDT", *Adv. Nano Res.*, **7**(2), 89-98. https://doi.org/10.12989/anr.2019.7.2.089.

Yazid, M., Heireche, H., Tounsi, A., Bousahla, A.A. and Houari, M.S.A. (2018), "A novel nonlocal refined plate theory for stability response of orthotropic single-layer graphene sheet resting on elastic medium", *Smart Struct. Syst.*, **21**(1), 15-25. https://doi.org/10.12989/sem.2018.68.6.661.

Younsi, A., Tounsi, A., Zaoui, F.Z., Bousahla, A.A. and Mahmoud, S.R. (2018), "Novel quasi-3D and 2D shear deformation theories for bending and free vibration analysis of FGM plates", *Geomech. Eng.*, **14**(6), 519-532. https://doi.org/10.12989/gae.2018.14.6.519.

Zarga, D., Tounsi, A., Bousahla, A.A., Bourada, F. and Mahmoud, S.R. (2019), "Thermomechanical bending study for functionally graded sandwich plates using a simple quasi-3D shear deformation theory", *Steel Compos. Struct.*, **32**(3), 389-410. https://doi.org/10.12989/scs.2019.32.3.389.

Zenkour, A.M. and Abouelregal, A.E. (2014), "Decaying temperature and dynamic response of a thermoelastic nanobeam to a moving load", *Coupl. Syst. Mech.*, **3**(1), 1-16. https://doi.org/10.12989/acd.2018.3.1.001.

Zenkour, A.M. and Abouelregal, A.E. (2014), "The effect of two temperatures on a FG nanobeam induced by a sinusoidal pulse heating", *Struct. Eng. Mech.*, **51**(2), 199-214. https://doi.org/10.12989/sem.2014.51.2.199.

DC